

# GOMOS Level 2 evolution studies (ALGOM)

## Validation of GOMOS-ENVISAT satellite data in the Upper Troposphere – Lower Stratosphere region

WP 1.1

Technical note

**V.F. Sofieva, I. Ialongo, J. Tamminen, E. Kyrölä**

Finnish Meteorological Institute, Helsinki, Finland

### Abstract

In this technical note, we present the results of the validation of GOMOS (Global Ozone Monitoring by Occultation of Stars) Version 6 data in the UTLS (Upper Troposphere - Lower Stratosphere) region. GOMOS ozone profiles are compared to the collocated ozonesonde data from NDACC (Network for the Detection of Atmospheric Composition Change) network. The results show a strong ozone overestimation by GOMOS in the tropopause region and below (median relative difference up to 100%), particularly large in the tropics. The influence of retrieval uncertainties and star properties on the large observed bias in the troposphere is also investigated. No apparent correlation between the large bias and these parameters is found, thus preventing a simple data screening for getting a reliable data subset for UTLS studies. The comparison with climatological data also confirms these results.

We assessed also how known geophysical phenomena in the UTLS (seasonal cycles, influence of Asian Summer Monsoon) are reproduced by the GOMOS data. It is found that the UTLS phenomena are generally reproduced by the GOMOS V6 data at  $\sim 100$ hPa and above. At lower altitudes, spatio-temporal distributions obtained from GOMOS V6 data are not realistic.

The alternative retrievals by the AERGOM processor are also validated. AERGOM data have a smaller bias in the UTLS, but have a negative bias of  $\sim 5$ -10 % in the stratosphere above 30 km. Not all UTLS features are reproduced by the AERGOM data.

## 1 Introduction

This Technical Note describes the validation studies of GOMOS data performed within the ALGOM project, which is dedicated to development of advanced Level 2 GOMOS processing algo-

rithms. The WP 1 of this project is aimed at optimization of GOMOS retrievals in the UTLS. As a first part of the studies, the extensive validation of GOMOS data in the UTLS has been performed.

The lowest altitude of the GOMOS measurements depends on stellar brightness and the presence of clouds (Tamminen et al., 2010); it is usually between 5 and 20 km. The GOMOS V.6 data processing relies on the two-step inversion (Kyrölä et al., 2010): the spectral inversion and the vertical inversion. Since the aerosol extinction spectrum is not known a priori, a polynomial model is used for the description of the aerosol extinction in the GOMOS retrievals. In the early version of GOMOS processor (IPF 4.02), a simplified aerosol extinction model proportional to  $1/\lambda$  ( $\lambda$  is wavelength) has been used (Vanhellemont et al., 2005), while further developments (IPF 5.0 and IPF 6.0) use a second-degree polynomial model in  $\lambda$  for the description of the aerosol extinction in GOMOS retrievals (Kyrölä et al., 2010; Vanhellemont et al., 2010). The study by Tamminen et al. (2010) has shown that the retrieval of GOMOS ozone profiles in the UTLS is highly sensitive to the aerosol model. In particular, using higher order (2<sup>nd</sup> and 3<sup>rd</sup> order) polynomial aerosol models results in ~30% larger ozone values in the UTLS and in the troposphere compared to the lower order model (zero or 1<sup>st</sup> order).

The dedicated validation of GOMOS ozone profiles in the UTLS region have not been performed so far, although some results can be found in the extensive validation of GOMOS ozone profiles focused on the stratosphere. For IPF v.4.02, Meijer et al. (2004) reported a positive ozone bias ~20% in tropical UTLS in comparisons with ozonesondes. In comparisons with ozonesondes at two polar stations, Tamminen et al. (2006) found ~10 % bias for Sodankylä (67.4°N, 23.6°E) and over 20% negative bias for Marambio (64.3°S, 56.7°W) below 15 km. For GOMOS ozone profiles processed with IPF v.5.0, van Gijssel et al. (2010) have performed an analysis analogous to Meijer et al. (2004) but on a significantly larger dataset and found large GOMOS positive bias, over 40%, in the tropical UTLS and the troposphere. This conclusion is in full agreement with the validation work of Mze et al. (2010) using ozone soundings from 8 SHADOZ stations.

The validation of the latest GOMOS processor, IPF v.6, performed so far (which are also focused mainly on the stratospheric ozone) indicate, however, the presence of large GOMOS bias in UTLS. For example, Adams et al. (2014) reported over 20% positive GOMOS bias in UTLS in comparisons with OSIRIS/Odin v.5.0 profiles, which are of good quality in the UTLS (e.g., Cooper et al., 2011). Hubert et al. (2015) have performed validation of GOMOS v.6 profiles with ozonesondes and reported a large positive ozone bias in the UTLS and the troposphere nearly everywhere except at polar high latitudes (only winter-time measurements are available for these locations). Large positive GOMOS ozone biases in UTLS are also observed in data agreement tables created for the HARMOZ dataset (Sofieva et al., 2013), which consists of user-friendly vertically gridded ozone profiles from 6 limb-viewing instruments (GOMOS, MIPAS, SCIAMACHY, OSIRIS, SMR and ACE-FTS); the illustrations of the biases between the instruments are available at <http://www.esa-ozone-cci.org/?q=node/161>. The summary of GOMOS processors and the previous GOMOS validation in UTLS are summarized in Table 1.

Table 1. Summary of previous GOMOS ozone validation studies, with focus on UTLS.

Processor and its main features	Publication	Reference dataset	Main results in UTLS
IPF 4.02 - air density is retrieved - simplified aerosol model $1/\lambda$	Meijer et al. (2004)	ozonesondes, lidars	For tropical locations, a positive bias ~20 %
	Tamminen et al. (2006)	ozonesondes at Marambio and Sodankylä in 2003	For individual profiles, no clear UTLS biases. In statistics, +10 % bias for Sodankylä and over -20% for Marambio, altitudes below 15 km
IPF 5.0 - Air density is not retrieved but taken from ECMWF - A quadratic polynomial for modelling aerosols	Mze et al. (2010)	Ozonesondes from 8 tropical SHADOZ stations	Below the tropopause, a large positive bias (over + 50 %)
	van Gijssels et al. (2010)	Ozonesondes and lidars	For tropical locations, large positive bias over 40 %
IPF 6.0 - Improved calibration (in particular, characterization of dark charge) - "Full covariance matrix" in spectral inversion - Aerosols and air density are as in IPF 5.0	Adams et al. (2014)	OSIRIS v. 5.0x	GOMOS has strong positive bias >20%
	Hubert et al. (2015)	Ozone sondes	Large positive bias in the UTLS and the troposphere nearly everywhere except at polar high latitudes

The analyses presented in this TN are focused on ozone profiles. Aerosol data have been assessed in (Vanhellemont et al., 2010) and also within the dedicated project AERGOM. For ozone profiles, we have performed the validation in the UTLS region using collocated ozonesonde measurements. In our analysis, the position of the tropopause is taken into account. The influence of stellar properties and other parameters on quality of GOMOS ozone profiles in the UTLS is also investigated. In addition, we have also performed so-called "geophysical assessment" of the GOMOS ozone data. This geophysical assessment compares the spatio-temporal distributions in the UTLS with those obtained by other satellite instruments that have good data quality in the UTLS.

The Technical Note is organized as follows. In Section 2, we describe validation against collocated ozonesonde data. Section 3 is dedicated to geophysical assessment of GOMOS ozone profiles. In Section 4, the validation of the alternative GOMOS data processed within the framework of the AERGOM project is presented. Discussion and summary (Section 5) concludes the TN.

## 2 Validation using ozonesonde data

### 2.1 Data and the comparison method

GOMOS IPF Version 6 night-time ozone profiles (with solar zenith angles at tangent point larger than  $107^\circ$ ) from the full mission are used in this work. The GOMOS data have been screened for outliers according to the recommendations in the readme (file [http://earth.eo.esa.int/pes/envisat/gomos/documentation/RMF\\_0117\\_GOM\\_NL\\_\\_2P\\_Disclaimers.pdf](http://earth.eo.esa.int/pes/envisat/gomos/documentation/RMF_0117_GOM_NL__2P_Disclaimers.pdf)).

GOMOS ozone profiles are interpolated to 1 km vertical grid and compared to ozonesonde data from the NDACC network (extracted from [www.ndsc.noaa.gov](http://www.ndsc.noaa.gov)). Ozonesonde data have been smoothed down to the vertical resolution of GOMOS ozone profiles (which is 2 km below 30 km) and also interpolated to the same vertical grid. Figure 1 shows locations of the ground-based stations included in the comparison. Data availability is larger in the Northern Hemisphere (NH).

We selected GOMOS and ozonesonde data separated less than 1000 km in ground distance, less than  $3^\circ$  in latitude and less than 24 hours in time. The information about the number of collocated GOMOS profiles in UTLS and in the troposphere useful for the comparison with ozonesondes is collected in Table 2.

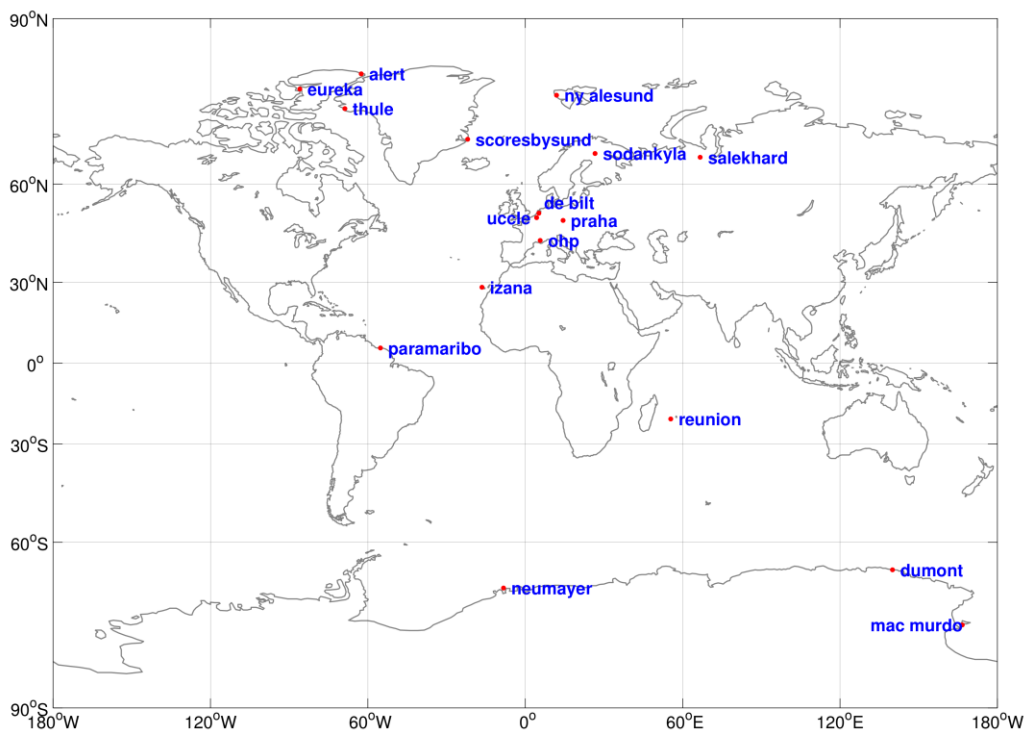


Figure 1. Locations of the NDACC ozonesonde stations considered in the comparison.

Table 2. Number of useful pairs of collocated GOMOS profiles and ozonesondes in UTLS and troposphere for the NDACC stations included in the comparison.

Station (Lat °N, Lon °E)	Number of collocations in UTLS	Number of collocations in troposphere
Alert (82.45, -62.51)	38	3
De Bilt (52.10, 5.18)	53	3
Dumont (-66.67, 140.02)	57	9
Eureka (79.99, -85.93)	51	3
Mac Murdo (-77.85, 166.63)	7	2
Izaña (28.30, -16.50)	160	67
Neumayer (-70.68, -8.26)	74	18
Ny Alesund (78.93, 11.93)	132	26
OHP (43.94, 5.71)	74	3
Paramaribo (5.8, -55.22)	75	15
Praha (50.00, 14.44)	66	0
Reunion (-21.06, 55.48)	82	34
Salekhard (66.50, 66.70)	7	0
Scorebysund (-70.68, -8.26)	112	20
Sodankylä (78.93, 11.93)	58	0
Thule (43.94, 5.71)	16	1
Uccle (50.80, 4.35)	195	6

For every collocated pair of profile, the tropopause height is determined based on the standard thermal lapse-rate criteria (WMO, 1957). The sonde temperature profiles are used for the tropopause detection. A detailed description of the tropopause height calculation can be found in e.g. (Sofieva et al., 2014).

In this work, the vertical range between 10 km above and 5 km below the tropopause height (referred to as UTLS hereafter) has been considered. The relative differences (RD, in %) between GOMOS ozone and the ozonesondes are derived as  $RD[\%] = 100 * (G - S) / S$ , where  $G$  refers to GOMOS and  $S$  to the ozonesonde ozone number density at each altitude.

## 2.2 Results

Figure 2 shows the relative difference between GOMOS ozone profiles and the ozonesondes data at different altitudes from all the stations presented in Figure 1. The color scale of the dots in Figure 2 indicates the GOMOS retrieval uncertainty (in %). When looking at the RD as a function of altitude (Figure 2, left), it can be noticed that the median RD is the largest below 15 km and any-

way smaller than 10%. This small value of the median RD is the result of the compensation between very large RD values with opposite sign obtained at different stations.

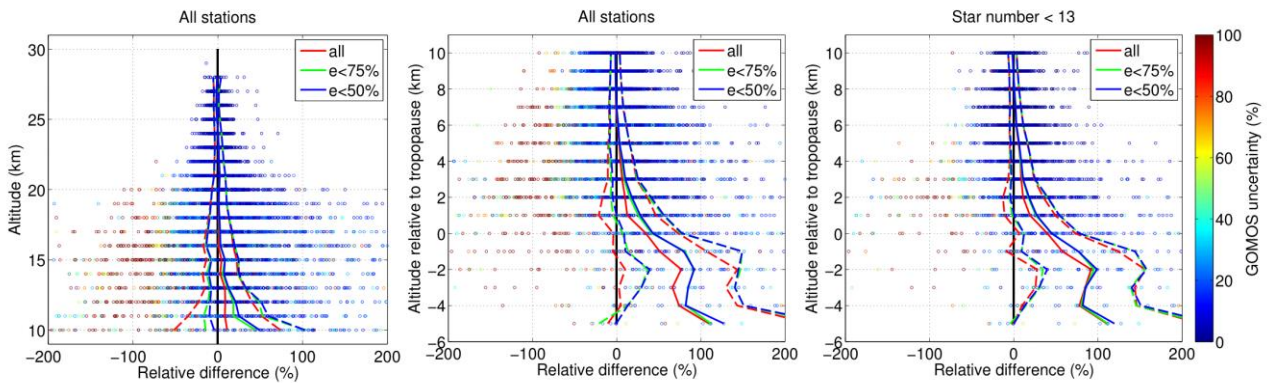


Figure 2. Percentage relative difference from collocations with all NDACC stations as a function of altitude (left panel) and altitude relative to the tropopause (centre) and for the 12 brightest stars (right). The color code of the points corresponds to the uncertainty of the GOMOS ozone retrieval. The lines indicate the median (solid) and the standard deviation (dashed) when the GOMOS uncertainties are smaller than 100% (red), 75% (green) and 50% (blue).

In order to separate the tropospheric and stratospheric components, the RD was plotted as a function of the altitude relative to the tropopause (Figure 2, center). Below the tropopause, a large ozone overestimation (median RD larger than 30%) by GOMOS can be observed.

Removing the GOMOS data with uncertainty larger than 75% or 50% (Figure 2, green and blue lines, respectively) does not reduce the large positive median RD values observed below the tropopause. In this case, the median RD is even larger than in the case with all data included in the comparison (red lines in Figure 2). This is because most of the data with large uncertainty corresponds to large negative RD values. The best accuracy in GOMOS retrievals can be achieved using the brightest stars (the smallest noise). When only the 12 brightest stars are taken into account (right panel in Figure 2), the difference between GOMOS and the ozonesondes becomes larger (median RD up to  $\sim 100\%$ ). The result is similar to the one obtained when the GOMOS data with large retrieval uncertainty were removed.

In order to evaluate the dependence of the observed bias on latitude, the relative difference as a function of the altitude relative to the tropopause was shown for different latitude regions (Figure 3). The largest overestimation is observed in the tropical region (Figure 3, bottom left), where also most of the data below the tropopause are available. The best agreement is found at high latitudes, especially for the stations in Antarctica (Figure 3, bottom right), where the median RD value is smaller than 40%. At the NH mid-latitudes a negative bias can be observed below the tropopause and  $\sim 3$  km above. No ground-based measurements are available at SH middle-latitudes. These results are in perfect agreement with those reported in the recent paper (Hubert et al., 2015).

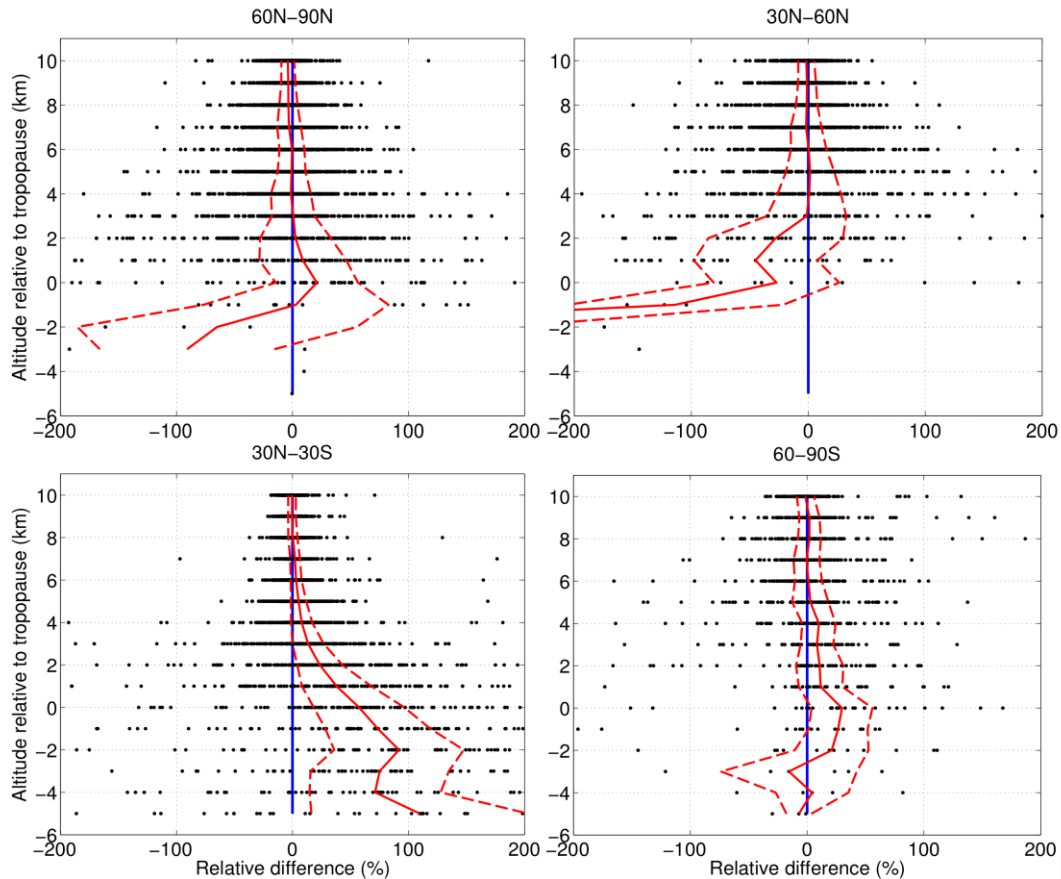


Figure 3 Relative difference of ozone profiles at different latitude bands (indicated in the title of each subplot). The red lines indicate the median (solid) and the standard deviation (dashed).

### 3 Geophysical assessment

In this section, we show how known geophysical phenomena in the UTLS are represented by the GOMOS v.6 data. Such analysis aimed at evaluation whether the useful information on UTLS can be obtained from GOMOS data.

#### 3.1 Comparison between GOMOS and ML climatology

Comparisons of GOMOS ozone profiles with collocated ozone sonde data have indicated a large positive bias in the UTLS and in the troposphere. Although we have used all available GOMOS data, the number of collocations with ozonesondes is limited, especially in the vertical region around the tropopause (Table 2). The GOMOS bias in UTLS is so large that it should be seen also at the climatological level. In order to confirm this, GOMOS observations have been compared with the new ozone climatology by McPeters and Labow (2012) referred to as ML climatology hereafter. The ML climatology is based on ozonesonde data (1988-2010) below 8 km (12 km at high latitudes) and Aura MLS ozone profiles (2004-2010) above 16 km (21 km at high latitudes), with a linear transition between these altitude ranges. The ML climatology presents monthly zonal mean

ozone mixing ratio profiles in  $10^\circ$  latitude zones from  $-90^\circ\text{S}$  to  $90^\circ\text{N}$  on pressure altitude levels from the ground to 66 km. The comparison of GOMOS data with ML climatology can indicate only a broad agreement, at climatological level. On the other hand, since it is based on all available data, the statistics is much more representative compared to comparisons based on collocated GOMOS and ozonesonde profiles.

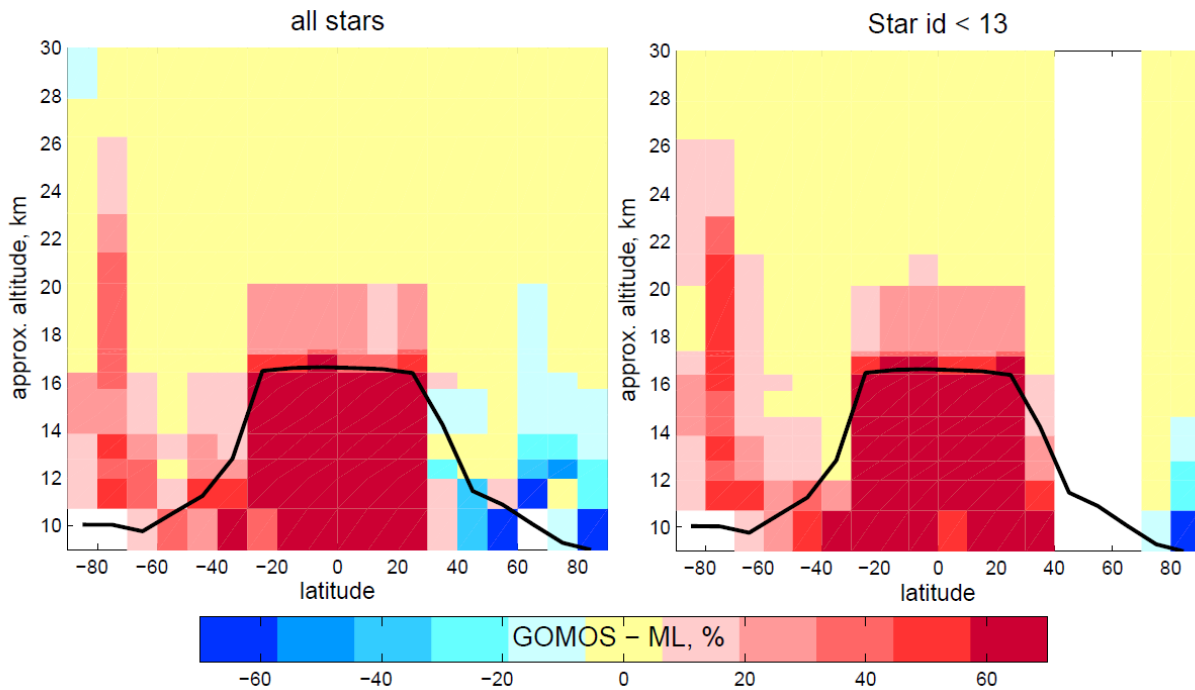


Figure 4. Relative difference between the yearly average GOMOS monthly zonal mean data and ML climatology for all stars (left) and for 12 brightest stars (right). The black line indicates the mean climatologic tropopause height.

For this comparison, the GOMOS number density ozone profiles have been converted to mixing ratio profiles using the ECMWF (European Centre for Medium-Range Weather Forecasts) air density profiles at occultation locations and presented on pressure grid. The monthly zonal mean values in  $10^\circ$  latitude zones from  $-90^\circ\text{S}$  to  $90^\circ\text{N}$  for years 2002-2010 have been compared with ML climatology.

Figure 4 (left) shows the relative difference between the yearly average GOMOS monthly zonal mean data and ML climatology, provided all valid GOMOS data are taken into account. Here the relative difference for each month is calculated and then averaged over all months. A strong overestimation ( $\sim 100\%$  and even more) of tropospheric ozone in the equatorial region is observed. At Northern Hemisphere middle latitudes (represented mainly winter months), GOMOS UTLS ozone is  $\sim 10\text{-}20\%$  lower than in the ML climatology, while at Southern Hemisphere high latitudes (also represented by winter months) it is  $\sim 10\text{-}20\%$  larger (in the zone  $70^\circ\text{S}\text{-}80^\circ\text{S}$ , up to 25km). These deviations at high and mid-latitudes might be related to non-uniform sampling by GOMOS measurements, while the very large overestimation of UTLS ozone abundances in tropics seems to



be related to the GOMOS processing. If only very bright stars are taken into account (Figure 4, right), the comparison with the ML climatology practically does not change. This confirms the results obtained in the comparison with the ozonesondes, i.e., that a large ozone overestimation is observed in the tropical troposphere for all stars. This does not allow selecting from the GOMOS dataset a subset of data with realistic ozone profiles in the UTLS region.

### 3.2 Influence of Asian Summer Monsoon

The Asian Summer Monsoon (ASM) contains a strong anti-cyclonic vortex in the UTLS, spanning from Asia to the Middle East. The ASM has been recognized as a significant transport pathway for water vapor and pollutants to the stratosphere (e.g., (Kunze et al., 2010; Park et al., 2007)). Figure 5 shows ozone distributions at 100 hPa in June-August from OSIRIS, ACE-FTS, MIPAS, and SCIAMACHY and GOMOS measurements. To obtain these maps, all available data have been used. The low ozone values in Asia associated with the strong upward motion of tropospheric air are clearly seen in the distributions by OSIRIS, ACE-FTS, MIPAS and SCIAMACHY. For GOMOS, the ozone values are overall larger at 100 hPa than for other instruments. However, low ozone values associated with the ASM are also observed in the GOMOS ozone distribution.

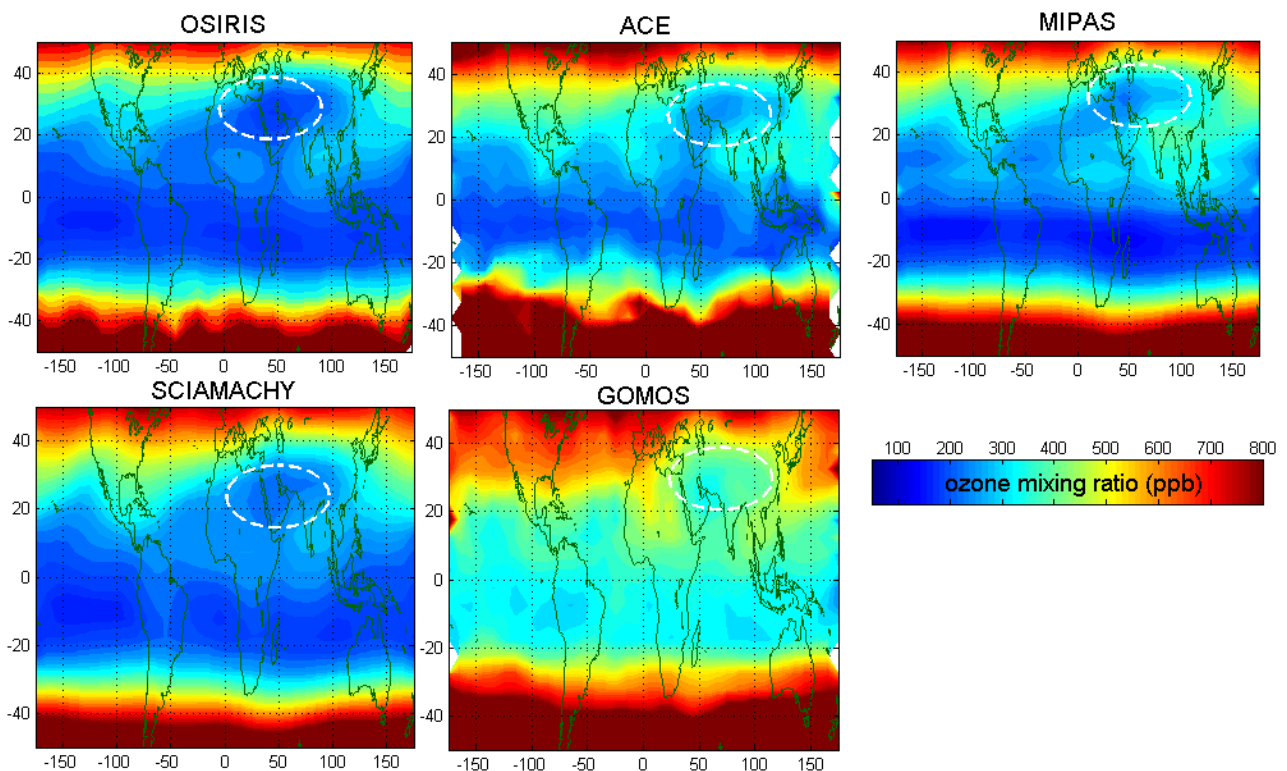


Figure 5. Mean ozone mixing ratio (ppb) at 100 hPa in the summer season (June-August), as inferred from all available measurements by OSIRIS, ACE-FTS, MIPAS, SCIAMACHY and GOMOS. Ellipses indicate low ozone values associated with the Asian Summer Monsoon.

### 3.3 Seasonal cycle in the tropical UTLS

A pronounced annual cycle is observed in the tropics with approximately factor-of-two variations in the strength of upwelling and temperature variations of up to 8 K, with faster upwelling and colder temperatures during boreal winter (e.g., (Randel and Jensen, 2013)). The tropical upwelling influences the vertical transport of trace constituents; this is especially important for ozone having a strong gradient across the tropical tropopause layer. The ozone annual cycle in the tropical UTLS, as observed by five satellite instruments is shown in Figure 6 (left). In this panel, the annual cycle from the ML ozone climatology is also shown. GOMOS data are positively biased, but the annual cycle is observed also in GOMOS data. The amplitude of the annual cycle (i.e., monthly mean data divided by the annual mean) is different between the datasets (Figure 6, right). For GOMOS, the amplitude of the annual cycle is smaller compared to those of MIPAS, OSIRIS and ML climatology. This might be the influence of the GOMOS sampling pattern or imperfect inversion.

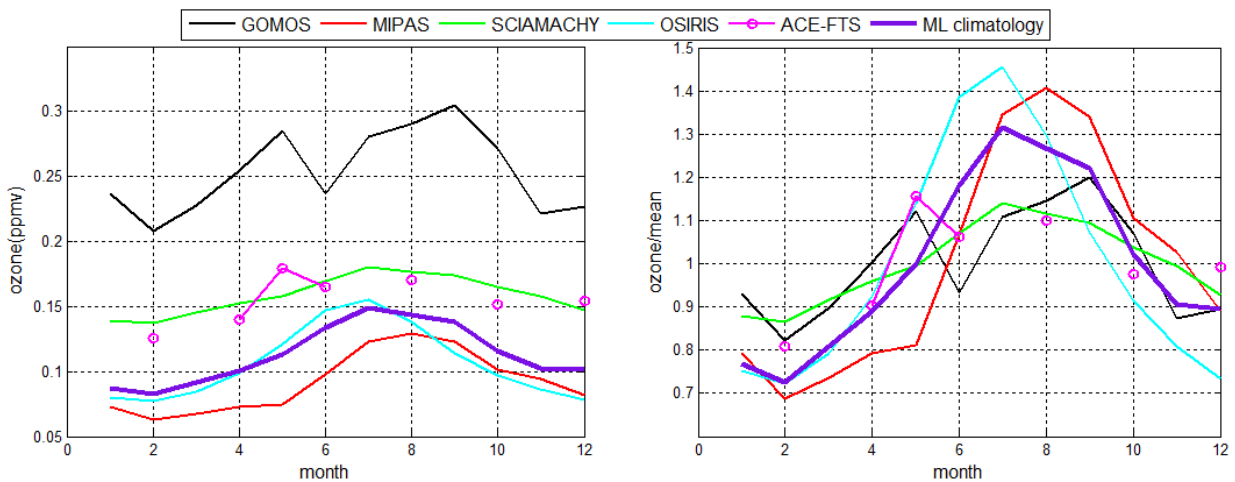


Figure 6. Center: ozone mixing ratio at 100 hPa from satellite instruments and ML ozone climatology (McPeters and Labow, 2012) (dashed purple line). Bottom: amplitude of annual cycle at 100 hPa for satellite instruments and ML climatology.

### 3.4 Seasonal cycle in the extra-tropical UTLS

The seasonal cycle of ozone at 100 hPa in the extra-tropics is mainly driven by the Brewer-Dobson circulation, with maxima observed in spring (e.g., (Hegglin et al., 2010)). Figure 7 shows the annual cycle at latitudes 40°N–60°N as observed by five satellite instruments and the ML climatology. To obtain these curves, all available satellite data are used. At 100 hPa, annual cycle curves for MIPAS, OSIRIS and SCIAMACHY agree perfectly with each other and with the ML climatology. ACE-FTS data also reproduce the seasonal cycle, but they are affected by low sampling. The annual cycle in the extratropical UTLS is observed also in GOMOS observed, with some deviations from the climatology (in particular, a slightly shifted phase). At 200 hPa, the annual cycles from MIPAS, SCIAMACHY, OSIRIS and ACE-FTS agree well with each other and with the ML climatology. In GOMOS data, the annual cycle at 200 hPa is not reproduced.

The analogous annual cycle, but for latitudes  $40^{\circ}\text{N}$ – $60^{\circ}\text{N}$ , is shown in Figure 8. For GOMOS, the same features as for the NH mid-latitudes are observed: at 100 hPa, GOMOS data reproduce satisfactorily the annual cycle, but at 200 hPa it does not.

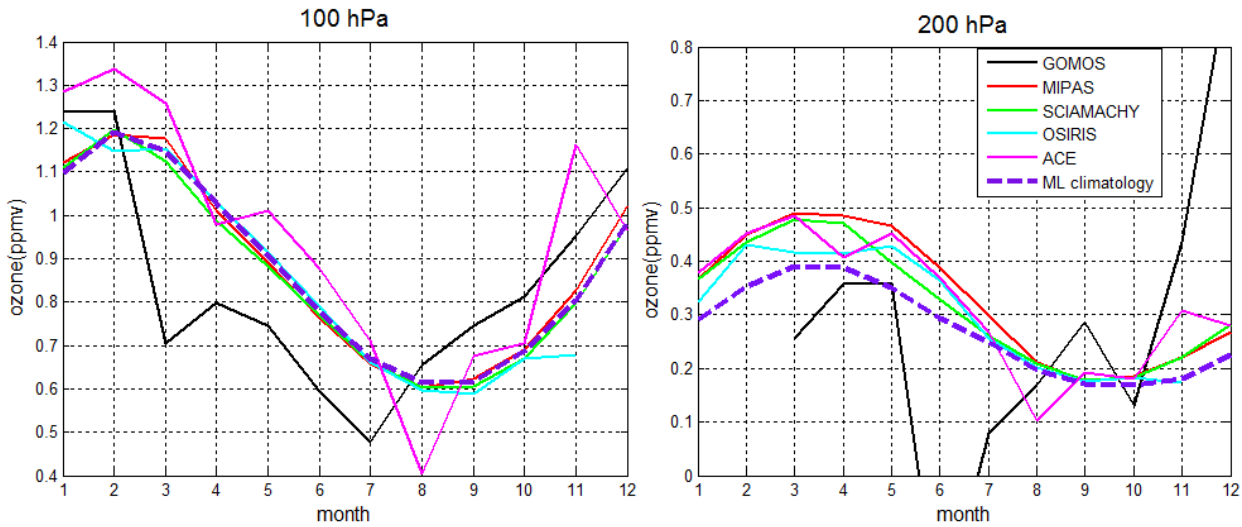


Figure 7. Annual cycle of ozone mixing ratio at  $40^{\circ}\text{N}$ – $60^{\circ}\text{N}$  from satellite instruments and the ML climatology, for 100 hPa (left) and 200 hPa.

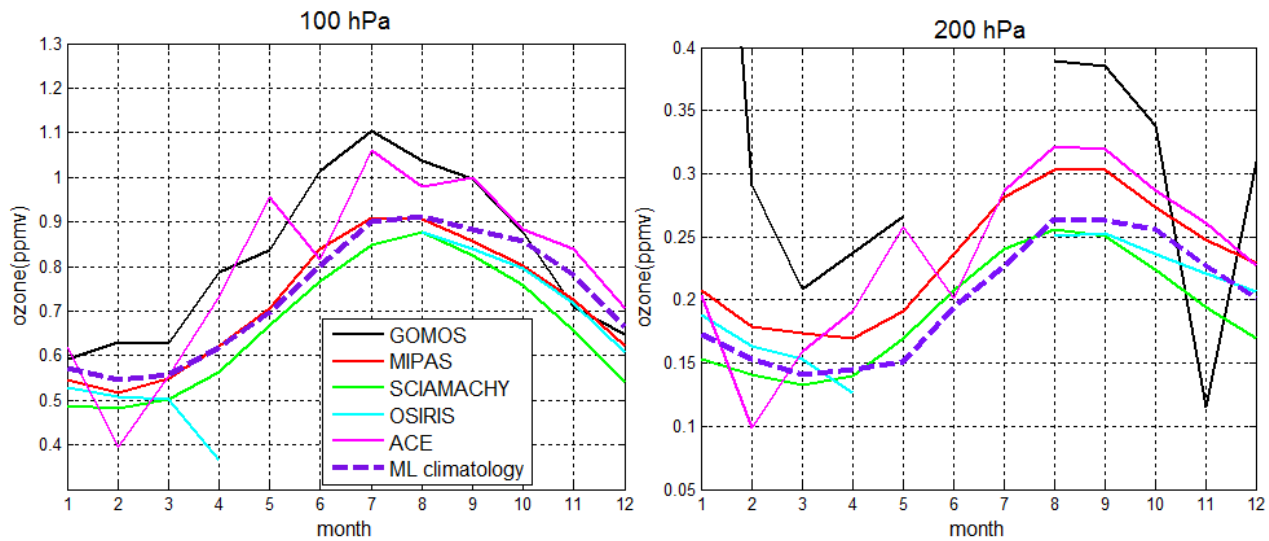


Figure 8. As Figure 7, but for  $40^{\circ}\text{S}$ – $60^{\circ}\text{S}$ .

### 3.5 Comparison of probability density functions

Probability density functions of geophysical parameters in some spatio-temporal periods provide a more detailed characterization of the parameter (compared to the commonly used characterization by the mean and the standard deviation).

As an illustration, we compared probability density function of ozone distribution in February at latitudes  $30^{\circ}\text{N}$ – $40^{\circ}\text{N}$ , where frequent stratospheric intrusions occur. Figure 9 shows probability density functions in the altitude range  $\sim 10$ – $40$  km for OSIRIS, MIPAS and GOMOS. In this figure, color indicates the fraction of data having a particular ozone partial pressure. As observed in

Figure 9, GOMOS has a larger fraction of data with high ozone abundances in the UTLS, compared to MIPAS and OSIRIS. Figure 10 shows the probability density functions, for the same instruments, at one pressure level 150 hPa. Compared to MIPAS and OSIRIS pdfs (which are in a very good agreement with each other), GOMOS reports larger probability of very small and very large data at this pressure level. This indicates the presence of significant noise in GOMOS data.

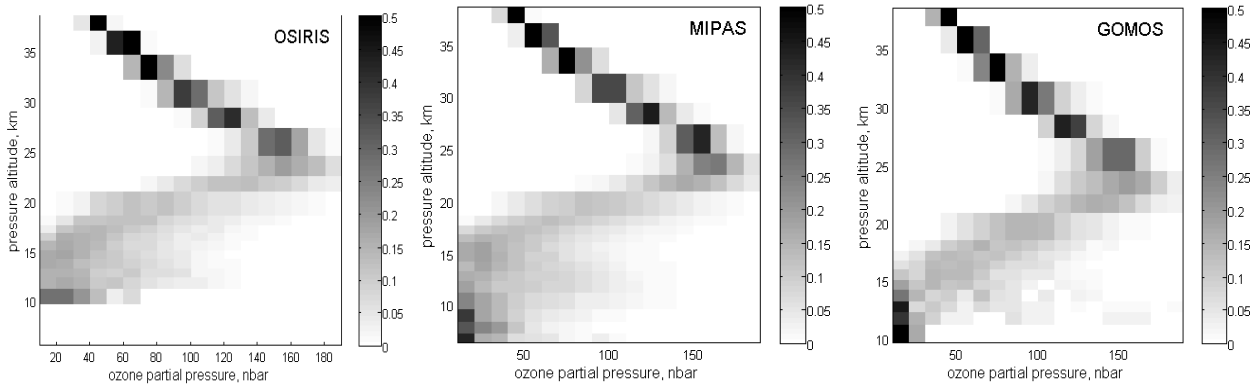


Figure 9. Probability density functions of ozone distributions, for OSIRIS, MIPAS, and GOMOS. Color indicates the fraction of the data.

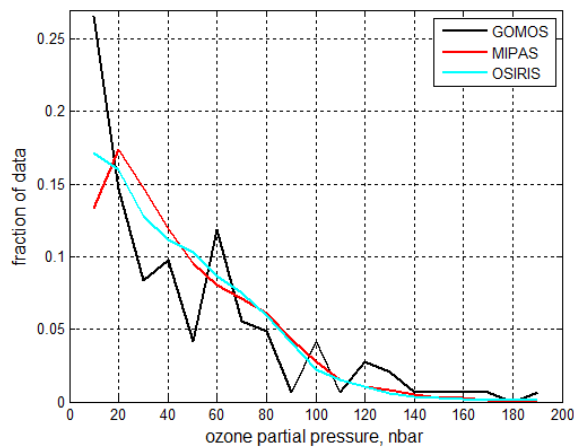


Figure 10. Probability density functions of ozone distribution at 150 hPa, for GOMOS, MIPAS and OSIRIS.

## 4 Assessment of AERGOM ozone data

There exist an alternative GOMOS ozone dataset developed within the framework of the AERGOM project and processed with algorithm, which is optimized for aerosol retrievals. It is expected that advanced characterization of aerosols should improve also ozone data in the UTLS. The AERGOM processor uses both spectrometer A and B data for retrievals of aerosol properties, full vertical inversion scheme, and a different (compared to V.6) regularization. In the AERGOM retrievals, the second degree polynomial model in  $1/\lambda$  is used for characterization of aerosol extinction spectra.

However, AERGOM processor is not optimized for ozone. Ozone profiles are with large oscillations, because almost no regularization is applied for ozone.

We have validated AERGOM ozone profiles against ozonesonde data. For the comparison, AERGOM ozone profiles were first smoothed down to the vertical resolution of IPF V6 data using the weighted-mean filter (weights are inversely proportional to uncertainties). Then all smoothed AERGOM ozone data are screened for invalid data according to GOMOS Disclaimer. The comparison with ozonesonde profiles has been performed in the same way as for V6 profiles.

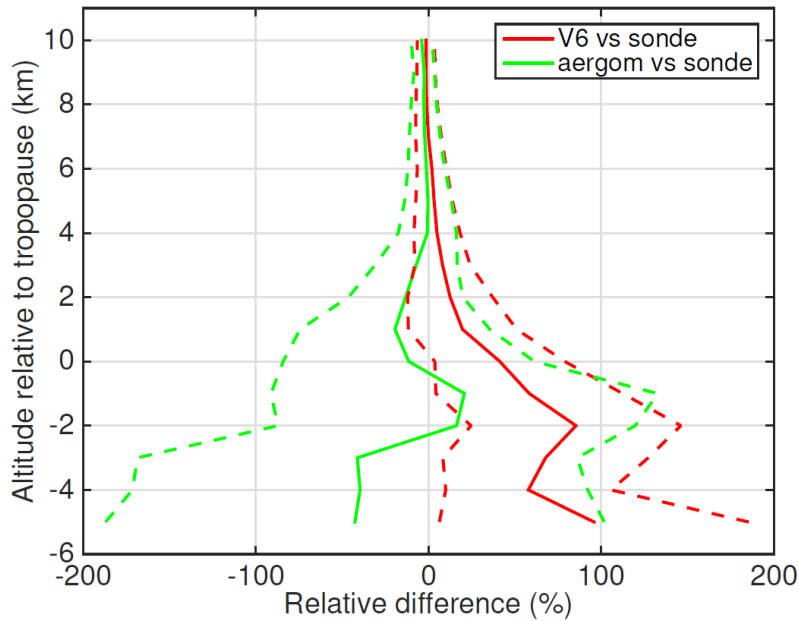


Figure 11. Relative difference of GOMOS and collocated ozonesonde profiles as a function of altitude relative to the tropopause. Red: IPF V6, green: AERGOM. Solid lines: median, dashed lines: standard deviation.

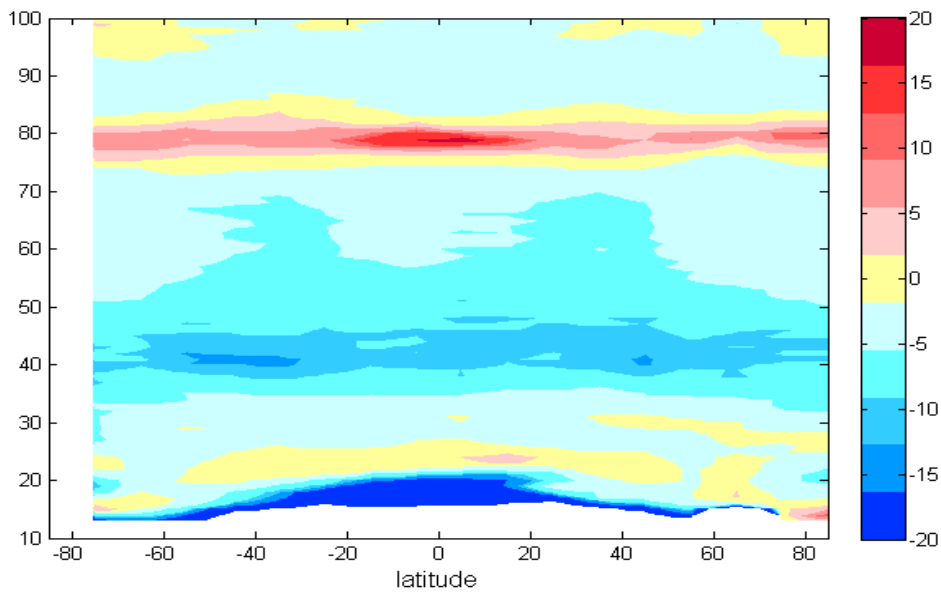
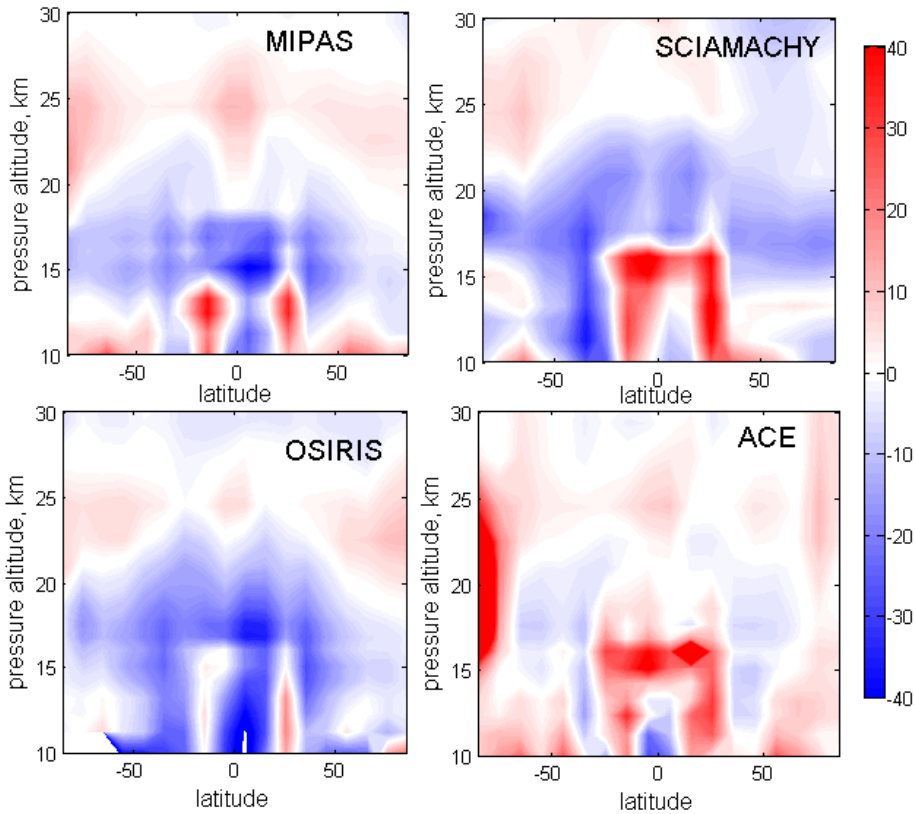


Figure 12. Color: the mean difference AERGOM-V6 (in %) as a function of altitude and latitude.

Figure 11 shows the statistics of differences (median, standard deviation) of GOMOS minus ozonesonde profiles as a function of altitude relative to the tropopause height. As expected, the bias is smaller in the AERGOM data. However, the standard deviation of the AERGOM ozone profiles is larger than in IPF V6 data, despite we smoothed the AERGOM data down to the vertical resolution of V6 profiles.

A



B

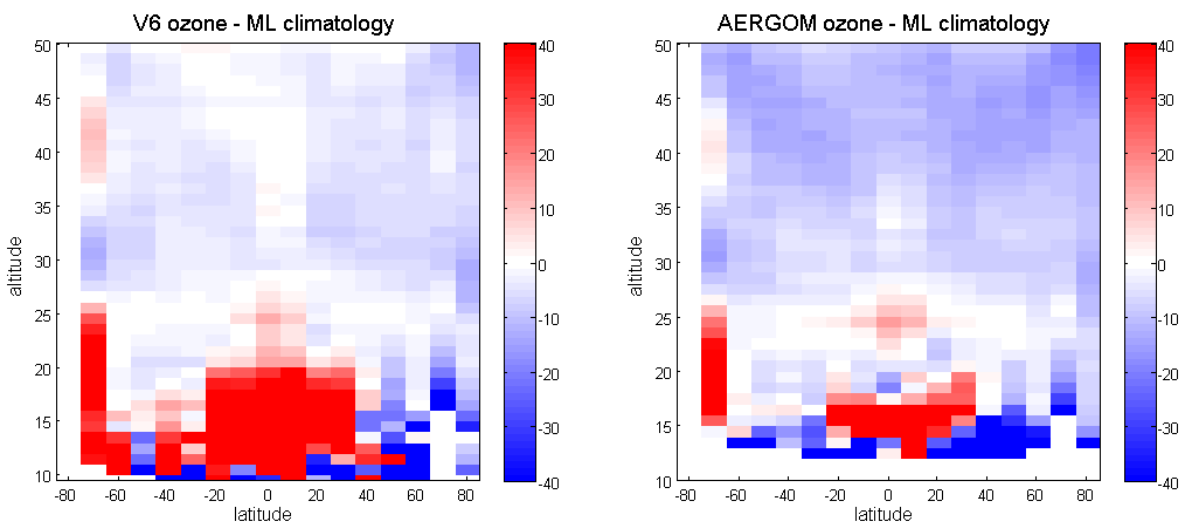


Figure 13. Deviations from ML climatology for year 2008 for MIPAS, SCIAMACHY, OSIRIS and ACE-FTS (panel A) and for GOMOS IPF V6 and AERGOM data (panel B).

It was found that AERGOM ozone profiles have significantly smaller (by 5-10 %) values in the stratosphere, above 30 km. This is unpleasant feature of AERGOM ozone profiles, because the V6 data are of very good quality in the stratosphere (van Gijssel et al., 2010; Hubert et al., 2015). Furthermore, the specific ozone UTLS enhancements in 2008 observed in deviations from ML climatology at  $\sim 20^{\circ}\text{N}$  and  $\sim 20^{\circ}\text{S}$  for MIPAS, SCIAMACHY, OSIRIS and ACE-FTS, are not seen in GOMOS AERGOM data, as well as in GOMOS V6 data.

## 5 Summary and discussion

The comparison of GOMOS V6 ozone profiles with collocated ozonesonde data has shown a strong overestimation (median relative difference up to 100%) of the ozone values by GOMOS in the tropopause region and below. The largest difference was observed in the tropics. Removing GOMOS data with large relative uncertainties does not reduce the median relative difference. The observed positive bias did not show any dependence on the star brightness, making impossible to select a subset of GOMOS dataset with realistic ozone profiles in the UTLS region.

The comparison of the GOMOS data with the ozone climatology by McPeters and Labow (2012) has confirmed the results of GOMOS comparisons with collocated ozonesonde profiles: GOMOS strongly overestimates UTLS ozone with large relative differences (up to more than 100%) observed in the tropics, and this bias is observed for all stars.

The geophysical assessment has shown that the main features in the UTLS are generally reproduced by the GOMOS V6 data at  $\sim 100$  hPa. At lower altitude, the spatio-temporal distributions obtained using GOMOS ozone data are often not realistic.

Alternative GOMOS data from the AERGOM processor has been also validated. AERGOM ozone profiles have a smaller bias in the UTLS in the comparisons with ozonesondes and the ML climatology. However, it was found a significant negative bias  $\sim 5-10$  % in the stratosphere (above 30 km) in the AERGOM data. In addition, not all geophysical features are reproduced by the AERGOM data. This does not allow using the AERGOM ozone profiles as advanced GOMOS data in the UTLS.

## 6 References

Adams, C., Bourassa, A. E., Sofieva, V., Froidevaux, L., McLinden, C. A., Hubert, D., Lambert, J.-C., Sioris, C. E. and Degenstein, D. A.: Assessment of Odin-OSIRIS ozone measurements from 2001 to the present using MLS, GOMOS, and ozonesondes, *Atmos. Meas. Tech.*, 7(1), 49–64, doi:10.5194/amt-7-49-2014, 2014.

Cooper, M., Martin, R. V, Sauvage, B., Boone, C. D., Walker, K. A., Bernath, P. F., McLinden, C. A., Degenstein, D. A., Volz-Thomas, A. and Wespes, C.: Evaluation of ACE-FTS and OSIRIS Satellite

retrievals of ozone and nitric acid in the tropical upper troposphere: Application to ozone production efficiency, *J. Geophys. Res. Atmos.*, 116(D12), doi:10.1029/2010JD015056, 2011.

Van Gijssel, J. A. E., Swart, D. P. J., Baray, J.-L., Bencherif, H., Claude, H., Fehr, T., Godin-Beekmann, S., Hansen, G. H., Keckhut, P., Leblanc, T., McDermid, I. S., Meijer, Y. J., Nakane, H., Quel, E. J., Stebel, K., Steinbrecht, W., Strawbridge, K. B., Tatarov, B. I. and Wolfram, E. A.: GOMOS ozone profile validation using ground-based and balloon sonde measurements, *Atmos. Chem. Phys.*, 10(21), 10473–10488, doi:10.5194/acp-10-10473-2010, 2010.

Hegglin, M. I., Gettelman, A., Hoor, P., Krichevsky, R., Manney, G. L., Pan, L. L., Son, S.-W., Stiller, G., Tilmes, S., Walker, K. A., Eyring, V., Shepherd, T. G., Waugh, D., Akiyoshi, H., Añel, J. A., Austin, J., Baumgaertner, A., Bekki, S., Braesicke, P., Brühl, C., Butchart, N., Chipperfield, M., Dameris, M., Dhomse, S., Frith, S., Garny, H., Hardiman, S. C., Jöckel, P., Kinnison, D. E., Lamarque, J. F., Mancini, E., Michou, M., Morgenstern, O., Nakamura, T., Olivié, D., Pawson, S., Pitari, G., Plummer, D. A., Pyle, J. A., Rozanov, E., Scinocca, J. F., Shibata, K., Smale, D., Teyssèdre, H., Tian, W. and Yamashita, Y.: Multimodel assessment of the upper troposphere and lower stratosphere: Extratropics, *J. Geophys. Res. Atmos.*, 115(D3), doi:10.1029/2010JD013884, 2010.

Hubert, D., Lambert, J.-C., Verhoelst, T., Granville, J., Keppens, A., Baray, J.-L., Cortesi, U., Degenstein, D. A., Froidevaux, L., Godin-Beekmann, S., Hoppel, K. W., Kyrölä, E., Leblanc, T., Lichtenberg, G., McElroy, C. T., Murtagh, D., Nakane, H., Russell III, J. M., Salvador, J., Smit, H. G. J., Stebel, K., Steinbrecht, W., Strawbridge, K. B., Stübi, R., Swart, D. P. J., Taha, G., Thompson, A. M., Urban, J., van Gijssel, J. A. E., von der Gathen, P., Walker, K. A., Wolfram, E. and Zawodny, J. M.: Ground-based assessment of the bias and long-term stability of fourteen limb and occultation ozone profile data records, *Atmos. Meas. Tech. Discuss.*, 8(7), 6661–6757, doi:10.5194/amtd-8-6661-2015, 2015.

Kunze, M., Braesicke, P., Langematz, U., Stiller, G., Bekki, S., Brühl, C., Chipperfield, M., Dameris, M., Garcia, R. and Giorgetta, M.: Influences of the Indian Summer Monsoon on Water Vapor and Ozone Concentrations in the UTLS as Simulated by Chemistry–Climate Models, *J. Clim.*, 23(13), 3525–3544, doi:10.1175/2010JCLI3280.1, 2010.

Kyrölä, E., Tamminen, J., Sofieva, V. F., Bertaux, J.-L., Hauchecorne, A., Dalaudier, F., Fussen, D., Vanhellefont, F., Fanton D'Andon, O., Barrot, G., Guirlet, M., Mangin, A., Blanot, L., Fehr, T., de Miguel, L. and Fraisse, R.: Retrieval of atmospheric parameters from GOMOS data, *Atmos. Chem. Phys.*, 10(23), 11881–11903, doi:10.5194/acp-10-11881-2010, 2010.

McPeters, R. D. and Labow, G. J.: Climatology 2011: An MLS and sonde derived ozone climatology for satellite retrieval algorithms, *J. Geophys. Res.*, 117(D10), D10303, doi:10.1029/2011JD017006, 2012.

Meijer, Y. J., Swart, D. P. J., Allaart, M., Andersen, S. B., Bodeker, G., Boyd, Braathena, G., Calisesia, Y., Claude, H., Dorokhov, V., von der Gathen, P., Gil, M., Godin-Beekmann, S., Goutail, F., Hansen, G., Karpetchko, A., Keckhut, P., Kelder, H. M., Koelemeijer, R., Kois, B., Koopman, R. M., Lambert, J.-C., Leblanc, T., McDermid, I. S., Pal, S., Kopp, G., Schets, H., Stubi, R., Suortti, T., Visconti, G. and and M. Yela: Pole-to-pole validation of ENVISAT/GOMOS ozone profiles using data from ground-



based and balloon-sonde measurements, *J. Geophys. Res.*, 109, D23305, doi:10.1029/2004JD004834, 2004.

Mze, N., Hauchecorne, A., Bencherif, H., Dalaudier, F. and Bertaux, J.-L.: Climatology and comparison of ozone from ENVISAT/GOMOS and SHADOZ/balloon-sonde observations in the southern tropics, *Atmos. Chem. Phys.*, 10(16), 8025–8035, doi:10.5194/acp-10-8025-2010, 2010.

Park, M., Randel, W. J., Gettelman, A., Massie, S. T. and Jiang, J. H.: Transport above the Asian summer monsoon anticyclone inferred from Aura Microwave Limb Sounder tracers, *J. Geophys. Res. Atmos.*, 112(D16), D16309, doi:10.1029/2006JD008294, 2007.

Randel, W. J. and Jensen, E. J.: Physical processes in the tropical tropopause layer and their roles in a changing climate, *Nat. Geosci*, 6(3), 169–176 [online] Available from: <http://dx.doi.org/10.1038/ngeo1733>, 2013.

Sofieva, V. F., Rahpoe, N., Tamminen, J., Kyrölä, E., Kalakoski, N., Weber, M., Rozanov, A., von Savigny, C., Laeng, A., von Clarmann, T., Stiller, G., Lossow, S., Degenstein, D., Bourassa, A., Adams, C., Roth, C., Lloyd, N., Bernath, P., Hargreaves, R. J., Urban, J., Murtagh, D., Hauchecorne, A., Dalaudier, F., van Roozendaal, M., Kalb, N. and Zehner, C.: Harmonized dataset of ozone profiles from satellite limb and occultation measurements, *Earth Syst. Sci. Data*, 5(2), 349–363, doi:10.5194/essd-5-349-2013, 2013.

Sofieva, V. F., Tamminen, J., Kyrölä, E., Mielonen, T., Veefkind, P., Hassler, B. and Bodeker, G. E.: A novel tropopause-related climatology of ozone profiles, *Atmos. Chem. Phys.*, 14(1), 283–299, doi:10.5194/acp-14-283-2014, 2014.

Tamminen, J., Karhu, J. A., Kyrölä, E., Hassinen, S., Kyrö, E., Karpechko, A. Y. and Piacentini, E.: GOMOS Ozone Profiles at High Latitudes: Comparison with Marambio and Sodankylä Sonde Measurements, in *Atmosphere and Climate SE - 5*, edited by U. Foelsche, G. Kirchengast, and A. Steiner, pp. 47–54, Springer Berlin Heidelberg, 2006.

Tamminen, J., Kyrölä, E., Sofieva, V. F., Laine, M., Bertaux, J.-L., Hauchecorne, A., Dalaudier, F., Fussen, D., Vanhellemont, F., Fanton-d'Andon, O., Barrot, G., Mangin, A., Guirlet, M., Blanot, L., Fehr, T., de Miguel, L. S. and Fraisse, R.: GOMOS data characterisation and error estimation, *Atmos. Chem. Phys.*, 10(19), 9505–9519, doi:10.5194/acp-10-9505-2010, 2010.

Vanhellemont, F., Fussen, D., Bingen, C., Kyrola, E., Tamminen, J., Sofieva, V. F., Hassinen, S., Verronen, P., Seppala, A., Bertaux, J.-L., Hauchecorne, A., Dalaudier, F., D'Andon, O. F., Barrot, G., Mangin, A., Theodore, B., Guirlet, M., Renard, J. B., Fraisse, R., Snoeij, P., Koopman, R. and Saavedra, L.: A 2003 stratospheric aerosol extinction and PSC climatology from GOMOS measurements on Envisat, *Atmos. Chem. Phys.*, 5, 2413–2417, 2005.

Vanhellemont, F., Fussen, D., Mateshvili, N., Tetard, C., Bingen, C., Dekemper, E., Loodts, N., Kyrola, E., Sofieva, V. F., Tamminen, J., Hauchecorne, A., Bertaux, J.-L., Dalaudier, F., Blanot, L., D'Andon, O. F., Barrot, G., Guirlet, M., Fehr, T. and Saavedra, L.: Optical extinction by upper

tropospheric/stratospheric aerosols and clouds: GOMOS observations for the period 2002-2008, Atmos. Chem. Phys., 10(16), 7997–8009, doi:10.5194/acp-10-7997-2010, 2010.